Valley formation and methane precipitation rates on Titan

J. Taylor Perron,[1] Michael P. Lamb,[1] Charles D. Koven,[2] Inez Y. Fung,[1] Elowyn Yager,[1] and Máté Ádámkovics[3]

[1] Branching valley networks near the landing site of the Huygens probe on Titan imply that fluid has eroded the surface. The fluid was most likely methane, which forms several percent of Titan's atmosphere and can exist as a liquid at the surface. The morphology of the valley networks and the nature of Titan's surface environment are inconsistent with a primary valley formation process involving thermal, chemical, or seepage erosion. The valleys were more likely eroded mechanically by surface runoff associated with methane precipitation. If mechanical erosion did occur, the flows must first have been able to mobilize any sediment accumulated in the valleys. We develop a model that links precipitation, open-channel flow, and sediment transport to calculate the minimum precipitation rate required to mobilize sediment and initiate erosion. Using data from two monitored watersheds in the Alps, we show that the model is able to predict precipitation rates in small drainage basins on Earth. The calculated precipitation rate is most sensitive to the sediment grain size. For a grain diameter of $1-10$ cm, a range that brackets the median size observed at the Huygens landing site, the minimum precipitation rate required to mobilize sediment in the nearby branching networks is $0.5-15$ mm hr^{-1}. We show that this range is reasonable given the abundance of methane in Titan's atmosphere. These minimum precipitation rates can be compared with observations of tropospheric cloud activity and estimates of long-term methane precipitation rates to further test the hypothesis that runoff eroded the valleys.

1. Introduction

[2] Images collected by the Huygens probe during its descent through Titan's atmosphere [*Tomasko et al.*, 2005] and during close approaches by the Cassini spacecraft [*Elachi et al.*, 2005; *Porco et al.*, 2005] have revealed the presence of drainage networks on the surface of Titan. Although a number of different network morphologies have been recognized, the most striking are the branching networks near the Huygens landing site [*Tomasko et al.*, 2005]. Given their similarity in form to terrestrial river networks [e.g., *Knighton*, 1998], it is likely that these networks were formed by a flowing fluid.

[3] Both the fluid and the substrate over which it flowed were quite different in composition from their terrestrial counterparts. Titan's low bulk density (1880 kg m^{-3}) is consistent with a crust composed mainly of water ice [*Schubert et al.*, 1986]. At Titan's surface temperature of 94 K, the brittle behavior of water ice at small scales is likely to be similar to that of rock on Earth: laboratory experiments indicate that the compressive [*Durham et al.*, 1983] and tensile [*Cuda and Ash*, 1984] strengths of ice at low temperatures approach those of granite at Earth's surface [*Goodman*, 1989]. Ground-based observations [*Gibbard et al.*, 1999; *Griffith et al.*, 2003] and data from the Cassini/Huygens mission [*Tomasko et al.*, 2005] suggest that bright regions on Titan's surface are composed of exposed water ice, likely containing hydrocarbon contaminants. Methane accounts for several percent of Titan's thick atmosphere, and near-surface temperatures and pressures are close to its triple point [*Kouvaris and Flasar*, 1991], so that Titan has a methane-based meteorological cycle that is similar in some respects to Earth's hydrologic cycle. The formation of short-lived methane clouds in Titan's troposphere [*Griffith et al.*, 2000, 2005; *Brown et al.*, 2002; *Roe et al.*, 2002] has been interpreted as evidence of liquid methane rain. The high concentration of atmospheric methane despite its short lifetime due to photolysis ($\sim10^7$ years [*Strobel*, 1982]) implies that the atmospheric reservoir is recharged by sources on the surface or in the interior [*Sotin et al.*, 2005; *Tobie et al.*, 2006]. The presence of drainage

---

[1]Department of Earth and Planetary Science and Center for Integrative Planetary Science, University of California, Berkeley, California, USA.

[2]Department of Environmental Science, Policy and Management, University of California, Berkeley, California, USA.

[3]Department of Astronomy and Center for Integrative Planetary Science, University of California, Berkeley, California, USA.

networks suggests that Titan's surface has been involved in this methane cycle.

[4] Few details are known about the frequency and magnitude of precipitation events on Titan, or about the processes that formed the drainage networks. In this paper, we describe the characteristics of the branching networks, consider several potential mechanisms for their formation, and show that the most likely mechanism is physical erosion by methane surface runoff. We then use a model that links precipitation, open-channel flow, and threshold sediment transport to estimate the minimum rate of methane precipitation required to form the branching networks.

2. Drainage Network Characteristics

[5] Images obtained by the Huygens Descent Imager/ Spectral Radiometer (DISR) during the probe's descent show that the region surrounding the probe's landing site consists of areas with distinct albedo contrasts [*Tomasko et al.*, 2005]. The low-albedo, branching drainage networks have formed on the higher-albedo terrain. Figure 1a shows a network that is resolved especially well by the images. Stereo processing of images taken at different times during the descent indicates that the center of the brighter terrain covered by branching networks in Figure 1a is elevated $100-200$ m above the darker terrain to the south [*Tomasko et al.*, 2005]. The stereo topography also shows that the dark networks are indeed valleys (i.e., topographic depressions). The networks appear to terminate at the boundary between the bright and dark terrains, which has been referred to as a "shoreline," although Huygens data, including images acquired at the surface (Figure 2), indicate that the dark lowland is not presently covered by liquid [*Tomasko et al.*, 2005; *Zarnecki et al.*, 2005]. Indeed, there is presently no evidence that any part of Titan's surface is covered by a large body of liquid [*West et al.*, 2005].

[6] Previous studies of Titan's surface have presented evidence that darker terrain is mantled with solid or liquid hydrocarbons deposited from the atmosphere, whereas brighter terrain is exposed water ice (with varying amounts of impurities) that presumably has been "washed clean" of hydrocarbons [*Griffith et al.*, 1991; *Smith et al.*, 1996; *Lorenz and Lunine*, 1997; *Gibbard et al.*, 1999; *Griffith et al.*, 2003; *Lorenz and Lunine*, 2005]. Although there are no detailed compositional data for the branching networks, it seems likely that their low albedo is due at least in part to the accumulation of hydrocarbon residue in the valleys. Roughness differences between the networks and adjacent terrain could also contribute to the albedo contrast. If the high albedo of the bright terrain surrounding the networks is due to incomplete mantling by hydrocarbon aerosols, it suggests that this terrain has been washed clean within the past 10^4-10^5 Earth years, the time required to produce (via photolysis in the atmosphere and subsequent gravitational settling) a dark surface coating a few hundred microns in thickness [*Lara et al.*, 1996; *Smith et al.*, 1996].

[7] The dark, branching features visible in the images may be wider and deeper than the portions that have most recently experienced fluid flow. By analogy with fluvial landforms on Mars [*Irwin et al.*, 2005] and Earth (e.g., the Colorado River and Grand Canyon), drainage channels on Titan may be significantly narrower and shallower than the

valleys they occupy. Throughout this paper, we use the term "valleys" to refer to the topographic depressions that correspond to the dark, branching features visible in the images and "channels" to refer to the inset topographic depressions within the valleys through which fluid flows.

[8] Figure 1a and the corresponding map in Figure 1b reveal several notable drainage network properties. As in most fluvial networks on Earth, valleys merge downstream to form a tributary network. Most of the valleys also appear to widen downstream. The undissected area between the heads of valleys that drain in opposite directions traces the approximate location of the main topographic divide in the elevated region, marked D in Figure 1b. By approximating the locations of other divides, it is possible to estimate the planform area that drains to a given point along a valley. For example, the shaded region in Figure 1b, which drains to point P, has a planform area of approximately 0.8 km^2. Other geometric properties of the valleys can also be derived from the images. The width of the valley, which must also be the maximum width of the channel, at point P is roughly 30 m. The horizontal distance from the estimated center of the elevated region (point C) to the shoreline (S) downstream of point P is roughly 3 km. Provided the sinuosity and profile concavity of the channel passing through point P are not large, the channel bed slope at point P probably lies between 0.03 and 0.07 (topographic relief of $100-200$ m divided by channel length of 3 km). The planform dimensions given here were initially measured from the image in Figure 1a, in which scale varies slightly with position, and later confirmed by comparison with the rectified images published by *Tomasko et al.* [2005].

[9] Given the limited image resolution (17 m pixel^{-1}) and the possibility that small surface features were obscured by Titan's atmospheric haze, the map in Figure 1b probably does not capture the fine structure of the drainage networks. The narrowest valleys visible in Figure 1a, which generally appear to originate within 100 m of topographic divides, are spanned by only a few pixels. Dissection of the bright highlands may be more extensive, with smaller valleys that are not resolved by the images extending farther upslope.

3. Erosion Mechanisms

[10] It is difficult to conclusively identify the processes that eroded the valley networks without detailed observations of morphology and channel evolution, but the available observations are sufficient to show that some processes are more likely than others. In this section, we consider the characteristics of the valley networks and Titan's surface environment, and comment on the feasibility of several possible formation mechanisms.

3.1. Thermal Erosion

[11] Thermal erosion (melting) of channels has been observed in glacial [e.g., *Marston*, 1983] and volcanic [e.g., *Swanson*, 1973] settings on Earth. Melting of pure water ice "bedrock" to form valleys is unlikely at Titan's low surface temperature. If hydrated compounds with lower melting temperatures (such as ammonia dihydrate, with a melting temperature of 176 K [*Fortes et al.*, 2003]) are present in significant amounts, it is possible that thermal
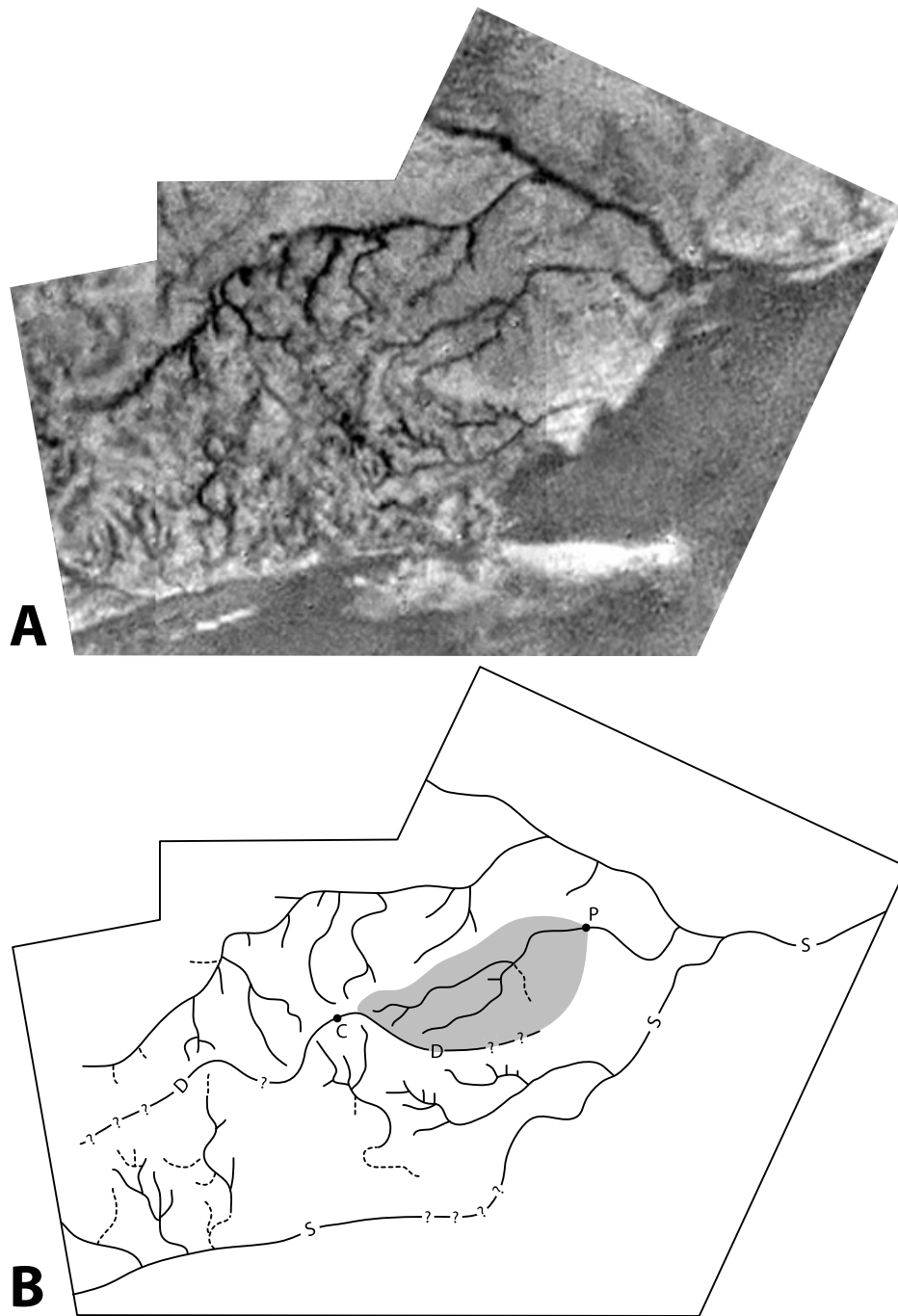
Figure 1. (a) Mosaic of three images acquired by the Huygens Descent Imager/Spectral Radiometer (DISR) at an altitude of 16 km. NASA Planetary Photojournal release PIA07236, courtesy of ESA/ NASA/JPL/University of Arizona. Scale varies, but the distance from the leftmost to the rightmost corner of the mosaic is approximately 6.5 km. Image resolution is approximately 17 m pixel^{-1}. Pixel values have been stretched to enhance contrast; the actual albedo difference between the lightest and darkest features is a factor of $\sim$3. (b) Map of the drainage network in Figure 1a. Solid lines trace the dark, sinuous features that have been shown to be valleys [*Tomasko et al.*, 2005]. Dotted lines trace possible valley paths. The line marked S is the "shoreline" separating the higher-albedo terrain dissected by the valleys from the lower-albedo terrain into which the valleys appear to drain. The line marked D shows the location of the main topographic divide as inferred from the drainage network, and point C marks the estimated location of the highest point along the divide. Uncertain portions of the drainage divide and shoreline are indicated with question marks. The shaded region shows the approximate extent of the area that drains to point P ($\sim$0.8 km^2). This drainage network is visible in Figures 1, 2, 5, 6, 7, 11, and 12 of *Tomasko et al.* [2005].
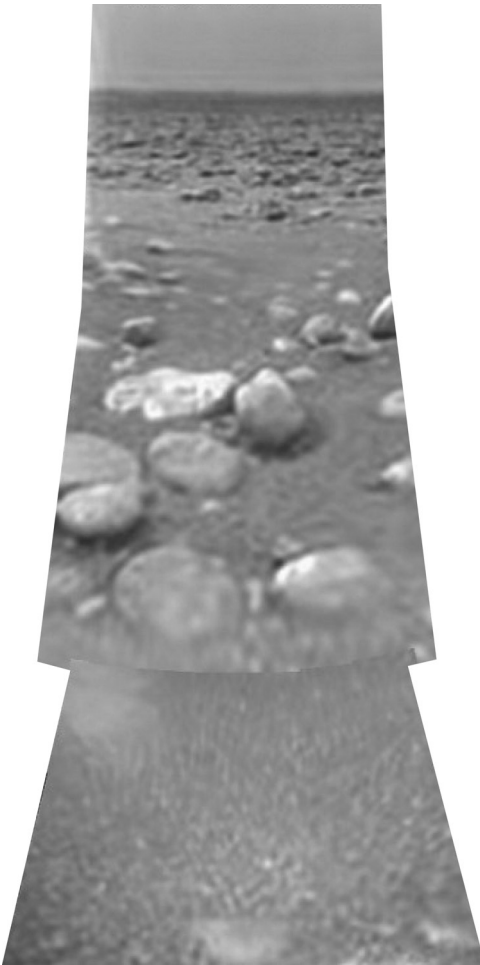
Figure 2. Merged Huygens DISR images of Titan's surface showing abundant sediment grains. Diameters of the largest grains in the foreground of the upper image are approximately 15 cm. Areas between these large grains appear to be dominated by centimeter-sized grains, although grains as small as 3 mm are resolved in the lower image, near the base of the probe. NASA Planetary Photojournal release PIA06440, courtesy of ESA/NASA/JPL/University of Arizona.

erosion by cryolavas has shaped Titan's surface. Melting of such compounds could conceivably have been facilitated by warming associated with a large impact event, a scenario that has been proposed for early Mars [*Segura et al.*, 2002].

[12] The morphology of the dendritic valley networks near the Huygens landing site is not consistent with formation by thermal erosion. Lava channels on Earth typically emanate from single eruptive centers, maintain constant width or narrow downstream as the lava cools and solidifies, and can branch downstream to form distributary networks [*Carr*, 1974; *Hulme*, 1974; *Griffiths*, 2000]. In contrast, the valleys in Figure 1 originate at many distributed sources, widen downstream, and have tributaries that merge into larger trunk streams. Solidification at the surfaces of channelized lava flows often forms discontinuous subterranean channels ("lava tubes") [*Griffiths*, 2000]. Both the images and the stereo topography [*Tomasko et al.*, 2005]

indicate that the dendritic valleys on Titan are continuous topographic depressions. Lava channels often terminate in deposits of solidified lava, yet there are no albedo features at the downstream ends of the valleys that could be interpreted as solidified flow fronts.

[13] Cryovolcanism on Titan may be ongoing [*Sotin et al.*, 2005], and cryovolcanic flow features may have formed elsewhere on the surface. Indeed, some Cassini Radar images show sinuous, flow-like features arranged radially on a circular feature that has been interpreted to be a cryovolcanic dome or shield [*Elachi et al.*, 2005], but the morphology of these features is distinct from those near the Huygens landing site.

3.2. Chemical Erosion

[14] Given the unfamiliar combination of surface materials on Titan, it is worth considering the possibility that the dendritic networks are dissolution features. *Lorenz and Lunine* [1996] use regular solution theory to calculate the solubilities of water and ammonia ices in methane and ethane as a function of temperature. Their results, which are consistent with experimental data on the solubility of water ice in nonpolar solvents [*Rest et al.*, 1990], suggest that dissolution erosion on Titan is possible but unlikely. The solubility of pure water ice in liquid methane or ethane at 94 K is so small ($<10^{-11}$ mole fraction) that only minor dissolution will occur over the age of the solar system [*Lunine and Stevenson*, 1985; *Lorenz and Lunine*, 1996]. The solubility of pure ammonia ice in liquid methane at 94 K may approach the solubility of calcium carbonate in water on Earth ($\sim10^{-5}$–10^{-6} mole fraction), though it could also be 3 orders of magnitude less within the uncertainty of the calculation. However, any ammonia at Titan's surface would be in the form of ammonia-water hydrates, for which solution properties are poorly understood. If the solubility of such compounds is intermediate between pure ammonia and pure water ice, then dissolution erosion should be quite slow even if the bright highlands in Figure 1a are composed entirely of ammonia hydrate. Mapping of Titan's surface composition is far from complete, but there is presently no spectral evidence of exposed ammonia.

[15] In terrestrial environments where dissolution causes significant erosion, there is often morphologic evidence of subsurface erosion. Karst terrain, in which surface runoff and groundwater have eroded carbonate bedrock, contains caverns, closed depressions, and discontinuous surface streams [*Summerfield*, 1991]. Although the images obtained during the Huygens descent are probably a very limited sample of the erosion features on Titan's surface, it is notable that there are no obvious karst-like features in the dendritic networks near the Huygens landing site.

3.3. Seepage Erosion

[16] On Earth, subsurface water from springs is known to erode loose sediment ("seepage erosion"), causing undercutting and failure of the ground surface ("sapping") [*Howard and McLane*, 1988; *Dunne*, 1990]. This leads to upslope retreat of the seepage face and the formation of a valley that often has short, stubby tributaries with amphitheater-shaped heads. The observation that some of the valleys near the Huygens landing site (not shown in Figure 1) appear to have short, stubby tributaries has led to sugges-

tions that seepage erosion played a role in their formation [*Tomasko et al.*, 2005; *Owen*, 2005]. Similar arguments have been made for some of the valleys on Mars [e.g., *Pieri*, 1976; *Mars Channel Working Group*, 1983].

[17] As *Tomasko et al.* [2005] observe, the morphology of the dendritic valley networks in Figure 1 is inconsistent with a seepage origin. The roughly radial drainage pattern indicates an isolated peak in the topography. Any springs at the heads of these valleys would have to be fed by artesian flow from a deep aquifer, and the locations of the valley heads imply that the sources of the springs would have to be very near the topographic divide. The many small tributaries imply a distributed source of fluid rather than a few localized sources of spring flow.

[18] Although this paper is primarily concerned with the dendritic networks, it is worth noting that the argument for seepage erosion based on the morphology of the stubbier valleys is problematic. Other processes, such as waterfall erosion, are known to produce stubby valley heads on Earth, especially in layered material [*Gilbert*, 1907; *Holland and Pickup*, 1976]. Furthermore, the feasibility of the seepage explanation depends on the strength of the material being eroded. For seepage erosion to occur in well-consolidated material (as opposed to loose sediment), the material must be sufficiently susceptible to weathering that the spring discharge can break it down into easily transportable debris [*Dietrich and Dunne*, 1993]. Case studies on Earth have shown that weakly cemented sedimentary rocks can be susceptible to seepage weathering [*Laity and Malin*, 1985; *Nash*, 1996], but the evidence for seepage erosion in more resistant lithologies is highly circumstantial and controversial [*Howard et al.*, 1994; *Craddock and Howard*, 2002; *Lamb et al.*, 2006]. Given the low solubilities of Titan's surface materials and the high mechanical strength of water ice at low temperatures [*Durham et al.*, 1983; *Cuda and Ash*, 1984], it seems unlikely that discharge from methane springs could weaken a well-consolidated substrate enough to allow seepage erosion to occur. Thus seepage erosion may be a viable mechanism for the formation of the stubby valleys on Titan only if the material being eroded is poorly consolidated.

3.4. Mechanical Erosion by Runoff

[19] Rivers on Earth most often erode bedrock mechanically through the action of the sediment they carry or by fluid discharge alone (for recent reviews, see *Whipple et al.* [2000], *Dietrich et al.* [2003], and *Whipple* [2004]). Sediment being transported over a bed of exposed bedrock can erode the bed as larger particles eject material during impacts, or through abrasion by smaller particles. Even in the absence of a significant sediment load, a river may erode its bed and banks by removing loosened joint blocks or through cavitation. *Collins* [2005] considers the feasibility of physical erosion mechanisms in methane flows on Titan and concludes that only cavitation is unlikely to play an appreciable role.

[20] The expectation that methane rainfall occurs on Titan introduces the possibility that the valleys were carved by rivers of methane fed by direct surface runoff, shallow (within a few tens of meters of the surface) groundwater flow, or both. Several properties of the drainage networks are consistent with this mechanism. The transport of dark material into topographic depressions (if this is indeed the source of the albedo contrast between the valleys and surrounding terrain) suggests surface runoff of some kind. As discussed in section 3.3, the proximity of valley heads to drainage divides and the development of valleys on what appears to be an isolated peak in the topography suggests that they are fed by an atmospheric source rather than by springs. Valleys that are farther from the drainage divide, and thus drain larger areas, are wider and more distinct. If these properties reflect the magnitude of fluid discharge through the valleys, then discharge increases with drainage area, as expected for flows fed by a surficial or atmospheric source [*Knighton*, 1998].

[21] In light of the observed characteristics of the dendritic valley networks and the nature of Titan's surface environment, mechanical runoff erosion is the least problematic of the mechanisms considered above. Of course, these mechanisms need not be mutually exclusive. For example, field observations of bedrock river incision on Earth indicate that even a small degree of chemical weathering can accelerate bedrock erosion [*Whipple et al.*, 2000; *Whipple*, 2004]. Thus, although there is no convincing evidence that dissolution is responsible for most of the erosion that formed the valleys on Titan, it could have been a contributing factor.

[22] One obvious test of the hypothesis that valley formation near the Huygens landing site has been dominated by mechanical runoff erosion would be to compare precipitation rates on Titan with those required to cause erosion of the surface. It may not be possible to complete this test at present, because neither time-averaged nor instantaneous rates of methane rainfall at Titan's surface are known with any certainty (see section 5.2 for a more detailed discussion). We can, however, estimate the minimum rate of methane rainfall required to initiate erosion in the observed valleys, and this is the subject of the next section. As our understanding of Titan's meteorology improves, this estimate will provide a quantitative basis for evaluating the extent to which rainfall has shaped Titan's surface.

4. Sediment Transport and Precipitation Rate

[23] The ground surface at the Huygens landing site is covered by clastic sediment ranging in diameter from 3 mm, the smallest grain size resolved by the DISR images, up to 15 cm [*Tomasko et al.*, 2005] (Figure 2). The Huygens Penetrometer appears to have struck one of the larger cobbles before penetrating into a soft subsurface with a strength consistent with unconsolidated sand-sized particles [*Zarnecki et al.*, 2005]. DISR surface reflectance spectra indicate that the sediment is probably composed of hydrocarbon-coated water ice [*Tomasko et al.*, 2005]. The rounding of the large particles in Figure 2 may have occurred during transport.

[24] The presence of erosional valleys and loose sediment on the surface of Titan provides a means of constraining the surface "hydrology" using remote observations. Bed sediment in a river channel acts as an armor, shielding the underlying bedrock against processes that cause mechanical erosion. If the valleys on Titan were eroded mechanically by surface runoff, the flow must first have been able to remove this armor by mobilizing any accumulated sediment cover-

ing the bed. Even if the valleys have formed in unconsolidated sediment rather than "bedrock," the erosion must have been accomplished by flows that were capable of entraining and transporting the sediment. By calculating the magnitude of the flow required to move bed sediment of a given size and relating the flow magnitude to the precipitation influx, we estimate the minimum precipitation rate required to erode the channel bed.

4.1. Precipitation and Runoff

[25] As precipitation falls on the surface at a rate P, some of it may infiltrate into the deep subsurface, and some may evaporate. The remainder will flow over the surface or through the shallow subsurface and eventually reach a drainage channel. At a location along the channel with upslope drainage area A and peak discharge Q,

$$cPA = Q. \qquad (1)$$

The coefficient c has a value between zero and unity and accounts for infiltration, evaporation, and attenuation of a rainfall pulse within a drainage basin. c can vary between locations with different substrates, drainage areas, and topographic contexts, and between precipitation events with different durations and magnitudes. For a rectangular channel with width w, flow depth h, and flow velocity u (averaged over the channel cross section),

$$Q = whu. \qquad (2)$$

[26] During an extended storm with steady state precipitation and runoff, infiltration and evaporation will approach zero as the ground becomes saturated and the relative humidity of the atmosphere approaches 100%, and c will approach unity. In practice, PA usually exceeds Q (i.e., $c < 1$) for two main reasons. First, infiltration and, to a lesser extent, evaporation can be appreciable during brief storm events. Second, the portion of a precipitation pulse that becomes runoff ("excess precipitation") is attenuated as it flows over the surface, through the shallow subsurface, and through the channel network [*Horton*, 1945; *Dunne*, 1978]. The result is that streamflow varies more slowly than precipitation, and the peak stream discharge following a precipitation pulse of finite duration is less than the product of the excess precipitation rate and drainage area. At present, we lack the detailed knowledge of Titan's surface and subsurface required to construct a rainfall-runoff model that predicts c [see, e.g., *Beven*, 2000; *Brutsaert*, 2005]. It is nonetheless worthwhile to use the first-order properties of drainage basins observed on Titan to estimate precipitation rates. In the sections that follow, we assume $c = 1$. This assumption is consistent with our goal of estimating a minimum precipitation rate, and in section 4.3, we show that our approach leads to only modest underestimates of precipitation rates over small, steep drainage basins on Earth.

[27] For steady, uniform flow of Newtonian fluids, the Darcy-Weisbach equation gives the flow velocity as

$$u = \sqrt{\frac{8gRS}{f}}, \qquad (3)$$

where g is the gravitational acceleration at Titan's surface (1.35 m s^{-2}), R is the hydraulic radius, equal to $wh/(w + 2h)$ for rectangular channels, S is the flow's surface slope, here assumed to be the same as the channel bed slope, and f is a dimensionless friction factor. In natural stream channels with alluvial beds, f depends primarily on the size of the bed sediment relative to the flow depth [e.g., *Hey*, 1983], and is independent of fluid viscosity provided the flow is fully turbulent (Reynolds number Re $= uR/\nu > 750$, with kinematic viscosity $\nu = 4 \times 10^{-7}$ m^2 s^{-1} for methane at 94 K). Combining equations (1)–(3) and using the definition of R, the precipitation rate is

$$P = \frac{1}{A} \frac{w^2 R}{w - 2R} \sqrt{\frac{8gRS}{f}}. \qquad (4)$$

4.2. Sediment Transport Threshold

[28] We now need an expression for the hydraulic radius of the shallowest flow that can mobilize the bed sediment. A considerable body of work in geomorphology (for a review, see *Buffington and Montgomery* [1997]) shows that the threshold for sediment transport occurs at a critical value of the Shields number, τ^* [*Shields*, 1936], which expresses the ratio of drag and lift forces exerted on a sediment grain to the submerged weight of the grain,

$$\tau^* = \frac{\rho RS}{(\rho_s - \rho)D}, \qquad (5)$$

where ρ is the density of the fluid, ρ_s is the density of the sediment, and D is the grain diameter. As written, equation (5) assumes that the only significant source of flow resistance is the roughness of the channel bed and walls. It also assumes that the density of the atmosphere is negligible compared to the fluid density, which is justified for Titan, where the density contrast is a factor of ~100 if the fluid is pure methane, and greater still if the fluid includes ethane. For hydraulically rough flow, particle Reynolds number Re$_p$ = $D\sqrt{gRS}/\nu > \sim500$, the critical value of the Shields number, τ_c^*, is roughly constant, with empirically determined values close to 0.05 [*Buffington and Montgomery*, 1997]. Several studies have shown, however, that when the sediment grain size is comparable to the flow depth (which we will see is characteristic of the flows considered here), τ_c^* approaches 0.1 [*Ashida and Bayazit*, 1973; *Mizuyama*, 1977; *Buffington and Montgomery*, 1997; *Shvidchenko and Pender*, 2000]. The critical Shields number is also a function of the channel slope [*Chiew and Parker*, 1994] and grain friction angle [*Kirchner et al.*, 1990], but for slopes up to 0.1 and friction angles of $\approx45°$, the difference is less than 10%. The scaling of sediment transport relations to conditions on Titan are discussed in greater depth by *Burr et al.* [2006].

[29] Solving equation (5) for R and substituting into equation (4) yields an expression for the minimum precipitation rate required to initiate sediment transport,

$$P_c = \frac{1}{A} \frac{w^2 \rho' \tau_c^* D}{wS - 2\rho' \tau_c^* D} \left(\frac{8\rho' g \tau_c^* D}{f} \right)^{\frac{1}{2}}, \qquad (6)$$

where $\rho' = \rho_s/\rho - 1$.

Table 1. Channel and Sediment Transport Parameters

Parameter	Rio Cordon	Erlenbach Torrent	Titan
Drainage area, A, km^2	5.0[a]	0.74[b]	0.8
Channel slope, S	0.13[a]	0.098	0.05
Channel width, w, m	5.6[a]	4.7	1–30
Darcy-Weisbach friction factor (f)	0.4[a]	3.0–9.8[c]	0.5[d]
Fluid density, ρ, kg m^{-3}	1000	1000	450[e]
Sediment density, ρ_s, kg m^{-3}	2650	2650	980
Critical Shields number, τ_c^*	0.1	0.1	0.1
Grain diameter, D, mm	117–174[a,c]	77–154[c]	1–1000

[a]*Lenzi et al.* [1999].
[b]*Rickenmann* [1997].
[c]Values of f and D for individual storms are given in Table 2.
[d]Value is for fully turbulent flows in which the diameter of large sediment grains $\approx$ flow depth [*Bathurst*, 1985].
[e]Value is liquid methane at 1.5 bar and 94 K.

[30] To clarify the dependence of P_c on the parameters in equation (6), we can make the approximation $R \approx h$ (accurate to within 10% for channels with $w/h > 18$) in equations (4) and (5), and equation (6) becomes

$$P_c = \frac{w}{AS}\left(\frac{8g}{f}\right)^{\frac{1}{2}}(\rho'\tau_c^*D)^{\frac{3}{2}}. \qquad (7)$$

In the sections that follow, equation (6) is used to calculate precipitation rates, because $R \approx h$ is not necessarily valid in all cases. Equation (7) serves only to illustrate, for wide channels, the sensitivity of P_c to the various parameters.

4.3. Validation With Terrestrial Data

[31] As noted in section 4.1, our approach is likely to underestimate the actual precipitation rate required to initiate sediment transport during a brief storm event. Monitoring of precipitation, streamflow, and sediment transport in drainage basins on Earth provides an opportunity to examine the magnitude of the discrepancy and confirm that our approach yields a useful estimate of the actual precipitation rate.

[32] The Rio Cordon, which drains a 5 km^2 watershed in the Dolomites, Italy, is the site of a monitoring experiment involving high-frequency measurements of precipitation, stream discharge, and bed and suspended load sediment transport [*Lenzi et al.*, 1999; *Lenzi*, 2004]. Similar monitoring efforts have been carried out in the 0.74 km^2 watershed of the Erlenbach Torrent, in the Swiss Alps [*Rickenmann*, 1997], and have recently been supplemented by bedload tracer studies [*Yager et al.*, 2005]. Sediment transport in the Rio Cordon takes place during large rainstorms in the summer or early fall, and occurs less than once per year on average. Sediment transport typically occurs many times throughout the year in the Erlenbach Torrent.

[33] Using the size of bed sediment transported during storms in these two watersheds, we calculated precipitation rates from equation (6) and compared these estimates with the measured rates. Parameter values are listed in Tables 1 and 2. For the Rio Cordon, we used data for three storm events between July 1989 and October 1993 reported by *Lenzi et al.* [1999]; for the Erlenbach Torrent, we used data from four storm events in the summer and early fall of 2004 collected by *Yager et al.* [2005] and the Swiss Federal Institute for Forest, Snow and Landscape Research (WSL).

[34] For channel beds composed of mixed grain sizes, it is necessary to select a representative grain diameter, D, to calculate the flow conditions. In many gravel bedded streams, there is evidence that the mobility thresholds of grains of all sizes occur at flows close to that required to move the median grain size, a condition known as equal mobility [*Parker et al.*, 1982]. In steep, rough streams like those considered here, with flow depths on the order of the largest grain diameter, bedload transport is more size-selective [e.g., *Lenzi et al.*, 1999]. Higher flows are observed to move large grains that remain immobile at lower flow conditions, and a progressively larger fraction of the bed material becomes mobile as flow increases. We therefore chose the diameter of the largest grain mobilized during a given event [e.g., *Baker and Ritter*, 1975; *Andrews*, 1983] as the representative value of D used to calculate the flow conditions in the Erlenbach Torrent and the Rio Cordon. Use of the maximum grain size relies on a

Table 2. Comparison of Observed and Predicted Discharges and Precipitation Rates

Date of Storm	D, mm	f[a]	Q_{obs}, m^3 s^{-1}	Q_{pred},[b] m^3 s^{-1}	P_{obs},[c] mm hr^{-1}	P_{pred}, mm hr^{-1}	c[d]	P_{obs}/P_{pred}
				Rio Cordon[e]				
3 July 1989	174	0.4	4.40	3.19	3.46	2.29	0.92	1.5
5 October 1992	117	0.4	2.86	1.71	5.96	1.25	0.35	4.8
2 October 1993	133	0.4	4.27	2.09	4.67	1.50	0.66	3.1
				Erlenbach Torrent				
24 July 2004	109	5.7	0.57	0.46	4.00	2.25	0.69	1.8
12 August 2004	77	9.8	0.27	0.21	6.42	1.00	0.20	6.4
26 August 2004	154	2.8	1.51	1.16	7.21	5.67	1.02[f]	1.3
24 September 2004	154	3.0	1.19	1.12	7.63	5.46	0.76	1.4

[a]Values of f for the Erlenbach Torrent are determined from equation (4) using measured values of R and u, and for the Rio Cordon from equations (3) and (4) of *Lenzi et al.* [1999].
[b]$Q_{pred} = P_{pred}A$.
[c]P_{obs} is the mean precipitation rate during the precipitation pulse immediately preceding the peak discharge.
[d]Values are from equation (1), $c = Q_{obs}/(P_{obs}A)$.
[e]Observed values are from *Lenzi et al.* [1999].
[f]Precipitation and discharge records for the 26 August event in the Erlenbach Torrent indicate that groundwater-fed baseflow generated by earlier rainfall events contributed to the peak discharge, leading to a c value greater than one.
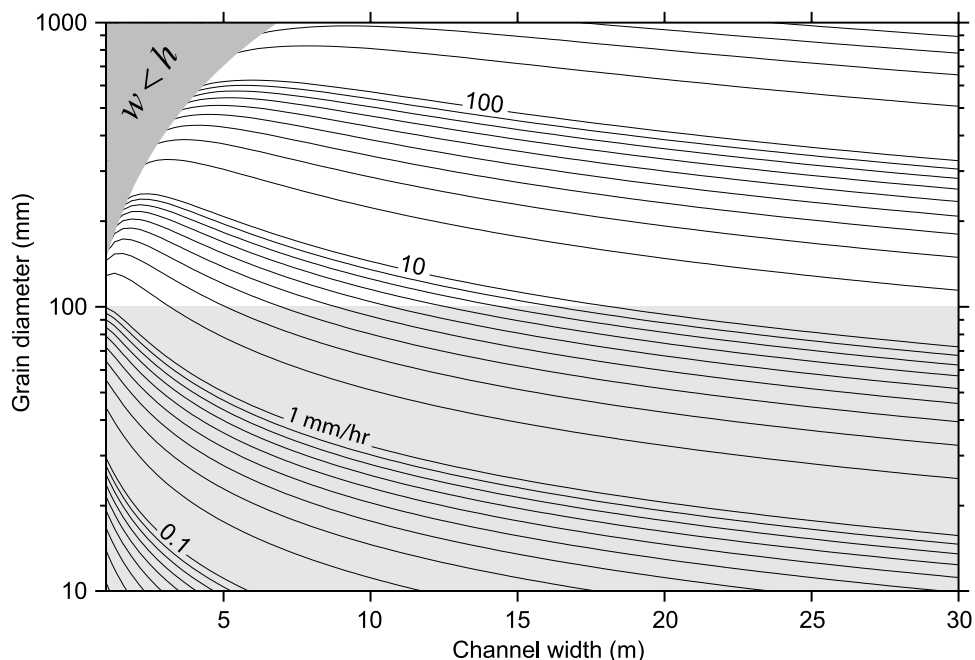
Figure 3. Contour map of the rate of methane precipitation (P_c) required to initiate sediment motion as a function of grain diameter (D) and channel width (w), calculated from equation (6). Contour units are millimeters per hour. The gray region in the upper left corresponds to parameter combinations for which flow depth exceeds channel width, a situation rarely observed in terrestrial rivers. The rectangular shaded region brackets the median grain diameter observed at the Huygens landing site (Figure 2).

measurement of the upper end of the grain size distribution, which may not be well sampled [*Komar and Carling*, 1991; *Wilcock*, 1992], but the potential errors are small for the purposes of our analysis. Because *Lenzi et al.* [1999] do not report the maximum grain size of the bedload, we substitute reported values of D_{90}, the grain diameter for which 90% of the bedload particles are smaller, for the storm events in the Rio Cordon. The grain size distribution of the bed material in the Rio Cordon suggests that the error introduced by this substitution could be up to a factor of 2.

[35] Table 2 summarizes the measured and predicted discharges and precipitation rates. Peak discharges are lower than the measured values, but by less than a factor of 2 in all cases. Two possible reasons for the underestimates of Q are (1) flows that were capable of transporting grains larger than the maximum grain size of the sampled bedload (particularly in the Rio Cordon, where D_{90} serves as a surrogate for the maximum grain size); and (2) additional sources of drag in the channels, such as bedforms, immobile or slowly moving boulders, and woody debris, that reduced the stress available for transporting sediment and raised the effective value of τ_c^* above 0.1. Predicted precipitation rates are lower than the measured rates by a factor of 3 or less in most cases. The discrepancy for each storm arises partly from the underestimate of Q, and (with the exception of the 24 August 2004 event in the Erlenbach Torrent) partly from a runoff coefficient, c, that is less than unity. Low c values are responsible for the larger underestimates of precipitation rates during the 5 October 1992 event in the Rio Cordon ($c = 0.35$) and the 12 August 2004 event in the Erlenbach Torrent ($c = 0.20$). Precipitation records indicate that these storms were characterized by brief precipitation pulses following relatively dry intervals, which suggests that the low c values reflect more pronounced infiltration into unsaturated ground in the early stages of the storms.

[36] These two test cases illustrate that the approach developed above can yield a useful estimate (within a factor of a few of the actual value) of precipitation rates over small, steep drainage basins on Earth. At present, there are few constraints on the properties of Titan's surface environment that affect runoff production, and so it is not possible to treat these terrestrial test cases as a calibration. There are, however, reasons to expect that our approach will perform similarly when applied to Titan. If the surface consists of intact ice rather than loose regolith, infiltration rates could be very low. With no vegetation to add flow resistance at the surface and promote infiltration, runoff and streamflow could be tightly coupled to precipitation.

4.4. Application to Titan

[37] Some of the parameters in equation (6) are known with less certainty for Titan than for Earth. The most critical of these is D, because possible values span more than an order of magnitude (Figure 2) and because the requisite precipitation rate is proportional to $D^{\frac{3}{2}}$. The second most critical parameter is w, because only the maximum channel width is constrained by Huygens images. Potential variations in the other parameters are sufficiently small that they will not affect the order of magnitude of our estimates. Using equation (6), we calculate P_c for 10 mm $< D <$ 1 m and 1 m $< w <$ 30 m (Figure 3). Values for other parameters are listed in Table 1.

[38] For the reasons noted above, the uncertainty in grain size results in a large range of calculated precipitation rates.

The dependence on channel width is comparatively weak, especially for $w > 10$ m (as equation (7) shows, it is approximately linear for large w/h). P_c ranges from < 0.1 mm hr^{-1} for a channel a few meters wide with 1 cm bed sediment to >500 mm hr^{-1} for a 30 m wide channel with 1 m boulders lining its bed. We narrow this range of estimates in section 4.5.

[39] The greater buoyancy of sediment particles on Titan implies that they will begin to move in shallower flows than on Earth (equation (5)), and this fact combined with the lower gravity implies that flow velocities at the sediment transport threshold will be lower on Titan than on Earth (equation (3)). Both of these effects reduce the discharge required to move sediment: for the same channel geometry, basin size, and bed sediment, the critical discharge on Titan is about one fourth of its terrestrial value.

[40] For the range of w and D in Figure 3, flow velocities range from 16 to 160 cm s^{-1}. Relative submergence (h/D) is between 2.3 and 3.3 for all but the largest particle diameters combined with the narrowest channel widths. Flow is Froude-subcritical ($u/\sqrt{gh} < 1$) in all cases. Re$_p$ ranges from 10^3 to 10^6, indicating hydraulically rough flow and justifying the assumption that τ_c^* is independent of Re$_p$ (and therefore also ν). Re ranges from 10^4 to 10^7, indicating fully turbulent flow and justifying the assumption that f is independent of Re (and therefore also ν).

[41] Throughout our analysis, we assume that the flows on Titan are composed entirely of liquid methane. If liquid ethane (with $\rho = 650$ kg m^{-3} and $\nu = 1.5 \times 10^{-6}$ m^2 s^{-1} at 1.5 bar and 94 K) forms part of the fluid, the enhanced sediment buoyancy would reduce the predicted precipitation rates. From equation (7), the size of this effect is at most a factor of 3.5. Although liquid ethane is several times more viscous than liquid methane, even flows composed entirely of ethane would be hydraulically rough and fully turbulent, rendering viscosity effects unimportant for the purposes of our calculation.

[42] If the diameter of the bed sediment is comparable to the flow depth, as it is in most of our solutions, the cross-sectional area of the flow may be less than wh, and the calculated flow discharge may be an overestimate. The errors involved are relatively small, however: In the worst-case scenario of sediment particles that protrude 100% from the bed surface, the difference is a factor of $1 - \pi D/4h$, or 26% for $h/D = 3$.

4.5. Sediment Grain Size Constraints

[43] To narrow the range of precipitation rate estimates, we can place further constraints on the sediment grain size. There are no images of the drainage networks capable of resolving sediment on the valley floors, but the surface sediment visible at the nearby Huygens landing site provides a useful reference. Size distributions derived from image-based grain counts by *Tomasko et al.* [2005] suggest that the median grain diameter of the surface layer in the immediate vicinity of the probe is ~5 cm. No grains larger than 15 cm are observed at the landing site, and no large boulders are apparent in images of the surrounding area obtained prior to landing.

[44] It is not known whether this sediment is of fluvial origin, although the rounding of large grains and moderate size sorting are consistent with fluvial transport. In addition,

low-altitude DISR images suggest that the clearing in the middle distance of Figure 2 may be a dry stream channel [*Tomasko et al.*, 2005]. If there is bed sediment in the steeply sloping channels 5 km to the north, it is reasonable to expect that it is at least as coarse as the material found on the nearly horizontal ground surface at the landing site. Although the largest transported grain size was used to estimate flow magnitudes in the terrestrial examples, transport of the largest grains is not necessarily required for erosion to occur. Provided the bed does not become completely armored by immobile particles, partial transport of the bed sediment and exposure of the bed could occur at lower flows. A size range of 1–10 cm, which encompasses most of the sediment grains observed at the landing site and is centered on the estimated median grain size, is the best available lower bound on the grain size in the channels within the branching valleys. As shown in Figure 3, this range corresponds to precipitation rates of 0.5–15 mm hr^{-1} for most channel widths.

5. Discussion
5.1. Interpretation of Precipitation Rates

[45] These precipitation rates provide an estimate of the minimum storm intensity required to mobilize sediment and initiate erosion of the channels. Our estimates are minima for several reasons. First, as noted in sections 4.1 and 4.3, infiltration, evaporation, and attenuation of the precipitation signal often result in peak stream discharges that are less than the precipitation flux PA ($c < 1$ in equation (1)). However, the example of the Erlenbach Torrent shows that these effects can be minimal during intense storms in small drainage basins. Furthermore, the evidence of channelized surface flow close to topographic divides on Titan (Figure 1) suggests that a significant fraction of the precipitation becomes runoff in channels via direct overland flow or shallow subsurface flow [*Dietrich and Dunne*, 1993].

[46] Second, precipitation fluxes and the resulting stream discharges may be significantly larger than the critical discharge required to initiate sediment transport. Indeed, flows in excess of the critical discharge would likely be required to cause appreciable bed erosion and to transport sediment out of the valleys. Here we have considered incipient grain motion as a minimum condition for any physical erosion mechanism (abrasion, plucking, or cavitation), and have not assessed the flow magnitudes required to cause significant erosion. The mechanics of sediment transport on Titan following entrainment are discussed by *Burr et al.* [2006].

5.2. Independent Constraints on Precipitation Rates

[47] Without information about the frequency and duration of storm events, the valley networks cannot be used to estimate long-term precipitation rates. Nor can we infer the time required to erode the channels; this would require an understanding of bedrock erosion mechanics that does not yet exist, even for terrestrial rivers. (See *Collins* [2005] for a discussion of the relative rates of bedrock river incision on Earth and Titan.) We can, however, consider whether typical precipitation events on Titan are intense enough to move the channel bed sediment.

[48] The most common clouds on Titan appear to be generated convectively as a result of surface heating. Even before the arrival of Cassini, clouds were observed to be forming over a large region surrounding the south pole [*Brown et al.*, 2002; *Roe et al.*, 2002] at altitudes of roughly 15 km. The extent of this region of cloud formation corresponds very closely to the area of maximum insolation, which suggests that cloud formation is driven by surface heating [*Brown et al.*, 2002; *Roe et al.*, 2002; *Bouchez and Brown*, 2005]. Observed cloud lifetimes as short as 2 hours have been interpreted as evidence that the condensed methane is raining out of the atmosphere [*Griffith et al.*, 2000, 2005]. From Cassini observations, *Griffith et al.* [2005] infer updraft velocities of $2-10$ m s^{-1} for clouds at middle southern latitudes. These are consistent with earlier theoretical predictions of updraft velocities in convective plumes, which range from 1 m s^{-1} [*Tokano et al.*, 2001a] to as much as 10 m s^{-1} [*Awal and Lunine*, 1994]. Although the region of apparent summer cloud activity does not currently cover the Huygens landing site, which is $10°$ south of the equator, it should pass over the site seasonally as the subsolar point alternates between the northern and southern hemispheres [*Brown et al.*, 2002; *Bouchez and Brown*, 2005]. If these convective clouds are capable of generating sufficient precipitation to move the sediment, the drainage networks could be active on an annual basis.

[49] The potential for convectively generated methane precipitation on Titan is considerable. If a parcel of air near the surface, with a methane mixing ratio of 2.9% [*Niemann et al.*, 2005] and a temperature of 93.7 K [*Fulchignoni et al.*, 2005], is lifted adiabatically to form a column stretching from the surface to the tropopause ($\sim$40 km), it will become supersaturated with respect to methane at altitudes above 8 km. This is consistent with altitudinal profiles of methane abundance measured by the Huygens probe Gas Chromatograph Mass Spectrometer, in which the mole fraction of methane is roughly constant between the surface and 8 km and declines sharply above this altitude [*Niemann et al.*, 2005]. If all methane vapor in excess of saturation is assumed to condense, the total depth of condensed methane in the troposphere will be 2.7 m. A more detailed explanation of this calculation is given in Appendix A. We used the same procedure to calculate the depth of condensed water (the so-called liquid water pathway, LWP) in Earth's atmosphere at tropical latitudes, where precipitation is dominated by convective storms. For a mixing ratio of 1.5% and a surface temperature of 295 K, the calculated LWP from the surface up to 10 km altitude is roughly 5 cm. This is slightly larger than airborne LWP measurements over tropical convective storms (up to $\sim$2 cm [*Olson et al.*, 1996]), but less than the LWP at the center of tropical cyclones ($\sim$10 cm (Experimental Tropical Cyclone Products from the NOAA-15, 16, 17 Advanced Microwave Sounder Units (AMSU), http://www.cira.colostate.edu/ramm/tropic/amsustrm.asp)). Thus we expect that 2.7 m is a reasonable upper bound on the condensed methane content of convective storm clouds on Titan. Using a more detailed model, *Tokano et al.* [2001a] predict that a convectively generated cloud will contain approximately 1 m of condensed methane (20 cm of liquid and 80 cm of graupel) per unit area. The difference arises in part because Tokano et al.'s dynamic model permits mixing with the surrounding atmosphere and

precipitation, both of which reduce the amount of condensed methane at higher altitudes.

[50] If 2.7 m of condensed methane were to rain out of the atmosphere over the shortest observed cloud lifetime of 2 hours, the resulting precipitation rate of 1.35 m hr^{-1} would exceed the rate required to transport 1 m boulders (Figure 3). This is several times greater than rates observed during the largest hour-long storms recorded on Earth ($0.2-0.4$ m hr^{-1} [*World Meteorological Organization*, 1994, p. 403]), but it is not inconsistent with the observed drainage network morphology. From equations (1)–(3), for example, a 30 m wide channel at point P in Figure 1b could convey this discharge with a flow depth of less than 5 m (probably much less, since the friction factor f will decrease as flow depth increases).

[51] Several factors could reduce the estimated precipitation rate. We have chosen the shortest observed cloud lifetime to obtain a maximum precipitation rate, but the condensed methane in a cloud could rain out over a longer interval. Voyager IRIS spectra suggest that the upper troposphere may be supersaturated in methane [*Courtin et al.*, 1995; *Samuelson et al.*, 1997; *Mayo and Samuelson*, 2005], perhaps because of a limited number of haze particles available to act as condensation nuclei [*Toon et al.*, 1988].

[52] Our precipitation estimate also assumes that all of the liquid methane reaches the surface without evaporating. The ventilating effect of air rushing past a falling raindrop can significantly enhance the rate of evaporation [*Beard and Pruppacher*, 1971; *Pruppacher and Rasmussen*, 1979], to the extent that even large drops may evaporate entirely before reaching the ground [*Lorenz*, 1993]. Applying the procedure of *Lorenz* [1993] to our calculated adiabatic profile, we find that drops with a diameter of 5 mm fall only 6 km below the cloud base before evaporating completely. Methane precipitation on Titan may only reach the surface when the cloud base altitude is low. *Barth and Toon* [2006] note, however, that raindrops with solid ethane cores will have higher density and therefore fall faster, and that the presence of dissolved N$_2$ in the drops should slow their evaporation. Alternatively, rain may reach the surface during storms of longer duration, in which the evaporation of drops that fall earlier in the storm increases the relative humidity at lower altitudes sufficiently to minimize the evaporation of subsequent drops [*Lorenz*, 2000]. The existence of such "rain shafts" would require sustained convective storms rather than the single rising airmass we have considered here. Note, however, that even a minor enhancement of relative humidity below the cloud base could be sufficient to allow sediment transport to occur: for the 1.35 m hr^{-1} maximum precipitation rate estimated above, only 0.003% (1.3%) of the precipitation leaving the clouds must survive the descent to produce a surface precipitation rate of 0.5 (15) mm hr^{-1}.

[53] Tropospheric convection on Titan may be vigorous enough to generate large storms, but they may be rare. The high atmospheric concentration of methane creates a large reservoir of latent heat available for enhancing the buoyancy of rising air parcels. This is particularly true if portions of the troposphere are supersaturated in methane. However, the energy dissipated by convective motions must ultimately be limited by the solar flux at Titan's surface, which

is small [*McKay et al.*, 1991]. Indeed, theoretical calculations suggest that moist convective plumes should cover at most 1% of the surface [*Awal and Lunine*, 1994; *Lorenz et al.*, 2005], a prediction that seems to agree well with the observed time-averaged cloud cover [*Bouchez and Brown*, 2005]. The frequency of storms could also be limited by the frequency of events that trigger convection. *Griffith et al.* [2000] show that the level of free convection, the altitude to which an air mass must ascend before the buoyancy enhancement due to methane condensation can sustain convection, on Titan is more than 5 km (for a surface relative humidity of 60%), compared with 1.5 km in the tropics on Earth. Given that the largest topographic features on Titan are unlikely to have relief in excess of several kilometers [*Perron and de Pater*, 2004], topographically triggered convection might be uncommon.

5.3. Frequency of Fluvial Activity

[54] A comparison of our calculated precipitation rates with estimated time-averaged precipitation rates for Titan allows us to speculate on the recurrence interval of storms large enough to initiate erosion in the channels. *Lorenz* [2000] predicts a maximum of 6 mm per Earth year based on an estimated rate of convective energy dissipation in the atmosphere. The 1-D cloud model of *Barth and Toon* [2006] predicts a precipitation rate of $\sim$2 mm yr^{-1}. The general circulation model of *Tokano et al.* [2001b] predicts globally averaged rates of up to 100 mm yr^{-1}. Using the range of $0.5-15$ mm hr^{-1} required to move $1-10$ cm sediment, and assuming that all precipitation falls during 2-hour storms that match the sediment transport threshold, erosion could occur as rarely as every 6 Earth years or as frequently as every day. A globally uneven precipitation distribution would imply that erosion could occur even more frequently where rain does fall, whereas coarser sediment or precipitation rates that exceed the sediment transport threshold would imply that erosion could be less frequent.

[55] Beyond the evidence that runoff has flowed over the elevated terrain recently enough to remove the cover of dark aerosols (i.e., within the last 10^5 years), the Huygens images provide no obvious clues as to how recently the drainage networks have been active. If the low albedo of the valleys is due to eolian accumulation of hydrocarbons, which seems possible in light of the detection of longitudinal dune fields by the Cassini Radar [*Lorenz et al.*, 2006; *Elachi et al.*, 2006], estimates of eolian transport rates could potentially be used to infer the time since flows last scoured the valleys. Alternatively, the low albedo could be the signature of an alluvial bed composed of hydrocarbon-coated sediment, as appears to be the case at the Huygens landing site [*Tomasko et al.*, 2005].

[56] Given the difficulty of detecting changes in the morphology of the drainage networks, cloud activity may be one of the best indicators of ongoing fluvial activity on Titan [*Schaller et al.*, 2006]. As more detailed observations of Titan's troposphere are made, it may become possible to use inferred microphysical properties of clouds and their time-dependent behavior to place upper bounds on the precipitation rate. The depth of liquid methane in a column of cloud with total optical thickness τ and effective droplet radius r is $\frac{2}{3}\tau r$. Assuming again that all condensed methane rains out over a 2-hour period and a droplet

size of 30 μm [*Griffith et al.*, 2005], a precipitation rate of 0.5 (15) mm hr^{-1} requires a cloud optical thickness of at least 50 (1500). Estimates of the optical thicknesses of short-lived midlatitude clouds by *Griffith et al.* [2005] are much smaller (<1).

[57] It is possible that the seasonal, convective clouds do not generate precipitation with an intensity sufficient to cause erosion in the channels, and that some other atmospheric phenomenon is responsible. Some observations hint at the occurrence of large, infrequent storms that dwarf the summer clouds. Major cloud outbursts have been inferred from disk-averaged spectra [*Griffith et al.*, 1998] and observed in images [*Schaller et al.*, 2006; *Lemmon et al.*, 2004]. *Toon et al.* [1988] and *Barth and Toon* [2004] have argued that methane rain may occur without cloud formation, though it is not clear that such rain would be sufficiently intense to create flows capable of transporting sediment in the channels.

[58] Stationary clouds observed outside the region of maximum insolation suggest that rainclouds may form over certain geographic features on the surface [*Griffith et al.*, 2005; *Roe et al.*, 2005b]. The low relief of the bright uplands near the Huygens landing site makes orographic cloud formation unlikely. The stationary clouds could also be a localized response to outgassing from a cryovolcanic eruption [*Roe et al.*, 2005a, 2005b; *Sotin et al.*, 2005]. Similar events may have occurred near the Huygens landing site in the past, but unless the bright uplands consist of unconsolidated material that is easily eroded, many eruptions would be required to form such prominent valleys.

6. Conclusions

[59] Morphologic properties of the dendritic valley networks and conditions at Titan's surface suggest that mechanical erosion by surface runoff is the primary mechanism that formed the valleys. Simple sediment transport calculations show that runoff erosion does not require unreasonably high precipitation rates, particularly in light of the considerable potential for convective motion and methane cloud formation in Titan's atmosphere. It seems likely that surface runoff plays a significant role in Titan's methane cycle.

[60] The current view of the methane cycle is too blurry, however, to provide a thorough test of the surface runoff hypothesis. Such a test will require answers to several outstanding questions: What are the frequency, magnitude and duration of precipitation events? What fraction of rainfall reaches the ground without evaporating? If and when rain does reach the ground, how is it partitioned between infiltration, evaporation and runoff? Future work should help to close this gap between inferences based on observations of surface features and our understanding of Titan's meteorology.

Appendix A: Calculation of Condensed Volatile Content in a Convective Plume

[61] To estimate the condensed volatile (water or methane) content of a convective plume, we assume that surface air with a mixing ratio w_0 and a temperature T_s is entrained and ascends rapidly to form a column reaching from the

surface (altitude $z = 0$) to the top of the troposphere ($z = Z$). Values of all parameters are given in Table A1. The pressure in the column, $P(z)$, is calculated by assuming a hydrostatic atmosphere with scale height z_* and surface pressure P_0,

$$P(z) = P_0 e^{-z/z_*}. \tag{A1}$$

The temperature $T(z)$ is obtained by integrating the dry adiabatic lapse rate in undersaturated conditions and the moist adiabatic lapse rate in saturated conditions [*Wallace and Hobbs*, 1977],

$$-\frac{dT}{dz} = \begin{cases} \dfrac{g}{c_P} & e_0 < \sigma e_{\text{sat}} \\ \dfrac{g}{c_P}\left(1 + \dfrac{L w_{\text{sat}}}{R_d T}\right)\left(1 + \dfrac{L^2 w_{\text{sat}}}{c_P R_v T^2}\right)^{-1} & e_0 \geq \sigma e_{\text{sat}} \end{cases}, \tag{A2}$$

with $T(0) = T_s$. Here g is gravitational acceleration, c_P is the specific heat capacity of dry air at constant pressure, L is the heat of condensation of the volatile, R_d and R_v are respectively the gas constants for dry air and the volatile species, σ is the saturation level above which condensation occurs (here assumed to be 100%), and e_0 is the vapor pressure corresponding to the surface mixing ratio w_0. Although the pressure-temperature conditions in the upper tropospheres of Earth and Titan permit the formation of solids, we neglect the effect of freezing on the temperature profile because the heat of fusion is roughly 10 times smaller than the heat of condensation for methane, and roughly 7 times smaller for water. The saturation mixing ratio w_{sat} is related to the saturation vapor pressure e_{sat} by

$$w_{\text{sat}} = \frac{e_{\text{sat}}}{P - e_{\text{sat}}}\frac{R_d}{R_v}, \tag{A3}$$

and e_{sat} is given by

$$e_{\text{sat}}(T) = e_{\text{ref}} \exp\left[\frac{L}{R_v}\left(\frac{1}{T_{\text{ref}}} - \frac{1}{T}\right)\right], \tag{A4}$$

where e_{ref} is a known saturation vapor pressure at a reference temperature T_{ref}. Equation (A4) is derived by integrating the Clausius-Clapeyron equation over T, assuming constant L. By analogy with equation (A3), the surface mixing ratio w_0 corresponds to a vapor pressure

$$e_0(P) = \frac{P w_0}{w_0 + \frac{R_d}{R_v}}. \tag{A5}$$

Using the ideal gas law, the total depth of condensed liquid (with density ρ) in the column is

$$\lambda = \frac{1}{\rho} \int_0^Z \frac{e'(z)}{R_v T(z)} dz, \tag{A6}$$

where

$$e'(z) = \begin{cases} 0 & e_0 \leq \sigma e_{\text{sat}} \\ e_0 - \sigma e_{\text{sat}} & e_0 > \sigma e_{\text{sat}} \end{cases}.$$

Table A1. Atmospheric Parameters

Parameter[a]	Earth (Water)	Titan (Methane)
w_0, kg/kg	0.015	0.029[b]
T_s, K	295	93.7[c]
Z, km	10	40
P_0, bar	1.01	1.47[c]
z_*, km	7.4	20.2
c_P, J kg^{-1} K^{-1}	1040	1040
L, J kg^{-1}	2.5×10^6	5.6×10^5
R_d, J kg^{-1} K^{-1}	287	303
R_v, J kg^{-1} K^{-1}	462	520
e_{ref}, bar	0.006	0.117
T_{ref}, K	273.2	90.7

[a]See text for definitions.
[b]*Niemann et al.* [2005].
[c]*Fulchignoni et al.* [2005].

For Earth's atmosphere, λ is often referred to as the liquid water pathway (LWP).

References

Andrews, E. D. (1983), Entrainment of gravel from naturally sorted river bed material, *Geol. Soc. Am. Bull.*, *94*, 1225–1231.

Ashida, K., and M. Bayazit (1973), Initiation of motion and roughness of flows in steep channels, paper presented at 15th IAHR Congress, Int. Assoc. of Hydraul. Eng., Istanbul, Turkey.

Awal, M., and J. I. Lunine (1994), Moist convective clouds in Titan's atmosphere, *Geophys. Res. Lett.*, *21*(23), 2491–2494.

Baker, V. R., and D. F. Ritter (1975), Competence of rivers to transport coarse bedload material, *Geol. Soc. Am. Bull.*, *86*, 975–978.

Barth, E. L., and O. B. Toon (2004), Properties of methane clouds on Titan: Results from microphysical modeling, *Geophys. Res. Lett.*, *31*, L17S07, doi:10.1029/2004GL019825.

Barth, E. L., and O. B. Toon (2006), Methane, ethane, and mixed clouds in Titan's atmosphere: Properties derived from microphysical modeling, *Icarus*, *182*, 230–250.

Bathurst, J. C. (1985), Flow resistance estimation in mountain rivers, *J. Hydraul. Eng.*, *111*, 625–643.

Beard, K. V., and H. R. Pruppacher (1971), A wind tunnel investigation of the rate of evaporation of small water drops falling at terminal velocity in air, *J. Atmos. Sci.*, *28*, 1455–1464.

Beven, K. J. (2000), *Rainfall-Runoff Modelling*, 360 pp., John Wiley, Hoboken, N. J.

Bouchez, A. H., and M. E. Brown (2005), Statistics of Titan's south polar tropospheric clouds, *Astrophys. J.*, *618*, L53–L56.

Brown, M. E., A. H. Bouchez, and C. A. Griffith (2002), Direct detection of variable tropospheric clouds near Titan's south pole, *Nature*, *420*, 795–797.

Brutsaert, W. (2005), *Hydrology: An Introduction*, 605 pp., Cambridge Univ. Press, New York.

Buffington, J. M., and D. R. Montgomery (1997), A systematic analysis of eight decades of incipient motion studies, with special reference to gravel-bedded rivers, *Water Resour. Res.*, *33*(8), 1993–2030.

Burr, D. M., J. P. Emery, R. D. Lorenz, G. C. Collins, and P. A. Carling (2006), Sediment transport by liquid surficial flow: Application to Titan, *Icarus*, *181*, 235–242.

Carr, M. H. (1974), The role of lava erosion in the formation of Lunar rilles and Martian channels, *Icarus*, *22*, 1–23.

Chiew, Y. M., and G. Parker (1994), Incipient sediment motion on non-horizontal slopes, *J. Hydraul. Res.*, *32*, 649–660.

Collins, G. C. (2005), Relative rates of fluvial bedrock incision on Titan and Earth, *Geophys. Res. Lett.*, *32*, L22202, doi:10.1029/2005GL024551.

Courtin, R., D. Gautier, and C. P. McKay (1995), Titan's thermal emission spectrum: Reanalysis of the Voyager infrared measurements, *Icarus*, *114*, 114–162.

Craddock, R. A., and A. D. Howard (2002), The case for rainfall on a warm, wet early Mars, *J. Geophys. Res.*, *107*(E11), 5111, doi:10.1029/2001JE001505.

Cuda, V., and R. L. Ash (1984), Development of a uniaxial ice tensile specimen for low temperature testing, *Cold Reg. Sci. Technol.*, *9*, 47–52.

Dietrich, W. E., and T. Dunne (1993), The channel head, in *Channel Network Hydrology*, edited by K. Beven and M. J. Kirkby, pp. 175–219, John Wiley, Hoboken, N. J.

Dietrich, W. E., D. Bellugi, A. M. Heimsath, J. J. Roering, L. Sklar, and J. D. Stock (2003), Geomorphic transport laws for predicting the form and evolution of landscapes, in *Prediction in Geomorphology*, *Geophys. Monogr. Ser.*, vol. 135, edited by P. R. Wilcock and R. M. Iverson, pp. 103–132, AGU, Washington, D. C.

Dunne, T. (1978), Field studies of hillslope flow processes, in *Hillslope Hydrology*, edited by M. J. Kirkby, pp. 227–294, John Wiley, Hoboken, N. J.

Dunne, T. (1990), Hydrology, mechanics, and geomorphic implications of erosion by subsurface flow, in *Groundwater Geomorphology: The Role of Subsurface Water in Earth-Surface Processes and Landforms*, edited by C. G. Higgins and D. R. Coates, *Spec. Pap. Geol. Soc. Am.*, *252*, 1–28.

Durham, W. B., H. C. Heard, and S. H. Kirby (1983), Experimental deformation of polycrystalline H_2O ice at high pressure and low temperature: Preliminary results, *J. Geophys. Res.*, *88*, 377–392.

Elachi, C., et al. (2005), Cassini Radar views the surface of Titan, *Science*, *308*, 970–974.

Elachi, C., et al. (2006), Cassini Radar's third and fourth looks at Titan, *Lunar Planet. Sci. Conf.*, *XXXVII*, abstract 1252.

Fortes, A. D., I. G. Wood, J. P. Brodholt, and L. Vocadlo (2003), The structure, ordering and equation of state of ammonia dihydrate ($NH_3 \cdot 2H_2O$), *Icarus*, *162*, 59–73.

Fulchignoni, M., et al. (2005), In situ measurements of the physical characteristics of Titan's environment, *Nature*, *438*, 785–791.

Gibbard, S. G., B. Macintosh, D. Gavel, C. E. Max, I. de Pater, A. M. Ghez, E. F. Young, and C. P. McKay (1999), Titan: High-resolution speckle images from the Keck Telescope, *Icarus*, *139*, 189–201.

Gilbert, G. K. (1907), The rate of recession of Niagara Falls, *U.S. Geol. Surv. Bull.*, *306*, 25.

Goodman, R. E. (1989), *Introduction to Rock Mechanics*, John Wiley, Hoboken, N. J.

Griffith, C. A., T. Owen, and R. Wagener (1991), Titan's surface and troposphere, investigated with ground-based, near-infrared observations, *Icarus*, *93*, 362–378.

Griffith, C. A., T. Owen, G. A. Miller, and T. Geballe (1998), Transient clouds in Titan's lower atmosphere, *Nature*, *395*, 575–578.

Griffith, C. A., J. L. Hall, and T. R. Geballe (2000), Detection of daily clouds on Titan, *Science*, *290*, 509–513.

Griffith, C. A., T. Owen, T. Geballe, J. Rayner, and P. Rannou (2003), Evidence for the exposure of water ice on Titan's surface, *Science*, *300*, 628–630.

Griffith, C. A., et al. (2005), The evolution of Titan's mid-latitude clouds, *Science*, *310*, 474–477.

Griffiths, R. W. (2000), The dynamics of lava flows, *Annu. Rev. Fluid Mech.*, *32*, 477–518.

Hey, R. D. (1983), Flow resistance in gravel-bed rivers, *J. Hydraul. Eng.*, *105*, 365–379.

Holland, W. N., and G. Pickup (1976), Flume study of knickpoint development in stratified sediment, *Geol. Soc. Am. Bull.*, *87*, 76–82.

Horton, R. E. (1945), Erosional development of streams and their drainage basins: Hydrophysical approach to quantitative geomorphology, *Geol. Soc. Am. Bull.*, *56*, 275–370.

Howard, A. D., and C. F. McLane (1988), Erosion of cohesionless sediment by groundwater seepage, *Water Resour. Res.*, *24*(10), 1659–1674.

Howard, A. D., W. E. Dietrich, and M. A. Seidl (1994), Modeling fluvial erosion on regional and continental scales, *J. Geophys. Res.*, *99*, 13,971–13,986.

Hulme, G. (1974), The interpretation of lava flow morphology, *Geophys. J. R. Astron. Soc.*, *39*, 361–383.

Irwin, R. P., R. A. Craddock, and A. D. Howard (2005), Interior channels in Martian valley networks: Discharge and runoff production, *Geology*, *33*(6), 489–492.

Kirchner, J. W., W. E. Dietrich, F. Iseya, and H. Ikeda (1990), The variability of critical shear stress, friction angle, and grain protrusion in water-worked sediments, *Sedimentology*, *37*, 647–672.

Knighton, D. (1998), *Fluvial Forms and Processes*, 400 pp., Oxford Univ. Press, New York.

Komar, P. D., and P. A. Carling (1991), Grain sorting in gravel-bed streams and the choice of particle sizes for flow-competence evaluations, *Sedimentology*, *38*, 489–502.

Kouvaris, L. C., and F. M. Flasar (1991), Phase equilibrium of methane and nitrogen at low temperatures —Application to Titan, *Icarus*, *91*, 112–124.

Laity, J. E., and M. C. Malin (1985), Sapping processes and the development of theatre-headed valley networks on the Colorado Plateau, *Geol. Soc. Am. Bull.*, *96*, 203–217.

Lamb, M. P., A. Howard, J. Johnson, K. Whipple, W. E. Dietrich, and T. Perron (2006), Can springs cut canyons into rock?, *J. Geophys. Res.*, *111*, E07002, doi:10.1029/2005JE002663.

Lara, L. M., E. Lellouch, J. J. López-Moreno, and R. Rodrigo (1996), Vertical distribution of Titan's atmospheric neutral constituents, *J. Geophys. Res.*, *101*, 23,261–23,283.

Lemmon, M., R. Lorenz, P. Smith, and J. Caldwell (2004), HST observations of Titan, 1994–1997: New surface albedo maps and detection of large-scale, sub-tropical cloud activity, *Geophys. Res. Abstr.*, *6*, 05783.

Lenzi, M. A. (2004), Displacement and transport of marked pebbles, cobbles and boulders during floods in a steep mountain stream, *Hydrol. Proc.*, *18*, 1899–1914.

Lenzi, M. A., V. D'Agostino, and P. Billi (1999), Bedload transport in the instrumented catchment of the Rio Cordon: Part I. Analysis of bedload records, conditions and threshold of bedload entrainment, *Catena*, *36*, 171–190.

Lorenz, R. D. (1993), The life, death and afterlife of a raindrop on Titan, *Planet. Space Sci.*, *31*, 647–655.

Lorenz, R. D. (2000), The weather on Titan, *Science*, *290*, 467–468.

Lorenz, R. D., and J. I. Lunine (1996), Erosion on Titan: Past and present, *Icarus*, *122*, 79–91.

Lorenz, R. D., and J. I. Lunine (1997), Titan's surface reviewed: The nature of bright and dark terrain, *Planet. Space Sci.*, *45*, 981–992.

Lorenz, R. D., and J. I. Lunine (2005), Titan's surface before Cassini, *Planet. Space Sci.*, *53*, 557–576.

Lorenz, R. D., C. A. Griffith, J. I. Lunine, C. P. McKay, and N. O. Rennò (2005), Convective plumes and the scarcity of Titan's clouds, *Geophys. Res. Lett.*, *32*, L01201, doi:10.1029/2004GL021415.

Lorenz, R. D., et al. (2006), Radar imaging of giant longitudinal dunes: Namib Desert (Earth) and the Belet Sand Sea (Titan), *Lunar Planet. Sci. Conf.*, *XXXVII*, abstract 1249.

Lunine, J. I., and D. J. Stevenson (1985), Evolution of Titan's coupled ocean-atmosphere system and interaction of ocean with bedrock, in *Ices in the Solar System*, edited by J. Klingeret al. pp. 741–757, Springer, New York.

Mars Channel Working Group (1983), Channels and valleys on Mars, *Geol. Soc. Am. Bull.*, *94*, 1035–1054.

Marston, R. A. (1983), Supraglacial stream dynamics on the Juneau Icefield, *Ann. Assoc. Am. Geogr.*, *73*, 597–608.

Mayo, L. A., and R. E. Samuelson (2005), Condensate clouds in Titan's north polar stratosphere, *Icarus*, *176*, 316–330.

McKay, C. P., J. B. Pollack, and R. Courtin (1991), The greenhouse and anti-greenhouse effect on Titan, *Science*, *253*, 1118–1121.

Mizuyama, T. (1977), Bedload transport in steep channels, Ph.D. thesis, Kyoto Univ., Kyoto, Japan.

Nash, D. J. (1996), Groundwater sapping and valley development in the Hackness hills, north Yorkshire, England, *Earth Surf. Processes Landforms*, *21*, 781–795.

Niemann, H. B., et al. (2005), The abundances of constituents of Titan's atmosphere from the GCMS instrument on the Huygens probe, *Nature*, *438*, 779–784.

Olson, W. S., C. D. Kummerow, G. M. Heymsfield, and L. Giglio (1996), A method for combined passive-active microwave retrievals of cloud and precipitation profiles, *J. Appl. Meteorol.*, *35*, 1763–1789.

Owen, T. (2005), Huygens rediscovers Titan, *Nature*, *438*, 756–757.

Parker, G., P. C. Klingeman, and D. G. McLean (1982), Bedload and size distribution in paved gravel-bed streams, *J. Hydraul. Div. Am. Soc. Civ. Eng.*, *108*, 544–571.

Perron, J. T., and I. de Pater (2004), Dynamics of an ice continent on Titan, *Geophys. Res. Lett.*, *31*, L17S04, doi:10.1029/2004GL019802.

Pieri, D. (1976), Distribution of small channels on the Martian surface, *Icarus*, *27*, 25–50.

Porco, C. C., et al. (2005), Imaging of Titan from the Cassini spacecraft, *Nature*, *434*, 159–168.

Pruppacher, H. R., and R. Rasmussen (1979), A wind tunnel investigation of the rate of evaporation of large water drops falling at terminal velocity in air, *J. Atmos. Sci.*, *36*, 1255–1260.

Rest, R. J., R. G. Scurlock, and M. F. Wu (1990), The solubilities of nitrous oxide, carbon dioxide, aliphatic ethers and alcohols, and water in cryogenic liquids, *Chem. Eng. J.*, *43*, 25–31.

Rickenmann, D. (1997), Sediment transport in Swiss torrents, *Earth Surf. Processes Landforms*, *22*, 937–951.

Roe, H. G., I. de Pater, B. A. Macintosh, and C. P. McKay (2002), Titan's clouds from Gemini and Keck adaptive optics imaging, *Astrophys. J.*, *581*, 1399–1406.

Roe, H. G., A. H. Bouchez, C. A. Trujillo, E. L. Schaller, and M. E. Brown (2005a), Discovery of temperate latitude clouds on Titan, *Astrophys. J.*, *618*, L49–L52.

Roe, H. G., M. E. Brown, E. L. Schaller, A. H. Bouchez, and C. A. Trujillo (2005b), Geographic control of Titan's mid-latitude clouds, *Science*, *310*, 477–479.

Samuelson, R. E., N. R. Nath, and A. Borysow (1997), Gaseous abundances and methane supersaturation in Titan's troposphere, *Planet. Space Sci.*, *45*, 959–980.

Schaller, E. L., M. E. Brown, H. G. Roe, and A. H. Bouchez (2006), A large cloud outburst at Titan's south pole, *Icarus*, *182*, 224–229.

Schubert, G. S., T. Spohn, and R. T. Reynolds (1986), Thermal histories, compositions and internal structures of the moons of the solar system, in *Satellites*, edited by J. A. Burns and M. S. Matthews, pp. 224–292, Univ. of Ariz. Press, Tucson.

Segura, T. L., O. B. Toon, A. Colaprete, and K. Zahnle (2002), Environmental effects of large impacts on Mars, *Science*, *298*, 1977–1980.

Shields, A. (1936), Anwendung der Aehnlichkeitsmechanik und der Turbulenzforschung auf die Geschiebebewegung, *Rep. 26*, 26 pp., Mitteil Preuss Versuchsanst. Wasserbau Schiffbau, Berlin. (Engl. transl. by W. P. Ott and J. C. van Uchelen, *Rep. 167*, 43 pp., Calif. Inst. of Technol., Pasadena.)

Shvidchenko, A. B., and G. Pender (2000), Flume study of the effect of relative depth on the incipient motion of coarse uniform sediments, *Water Resour. Res.*, *36*(2), 619–628.

Smith, P. H., M. T. Lemmon, R. D. Lorenz, L. A. Sromovsky, J. J. Caldwell, and M. D. Allison (1996), Titan's surface, revealed by HST imaging, *Icarus*, *119*, 336–349.

Sotin, C., et al. (2005), Release of volatiles from a possible cryovolcano from near-infrared imaging of Titan, *Nature*, *435*, 786–789.

Strobel, D. F. (1982), Chemistry and evolution of Titan's atmosphere, *Planet. Space Sci.*, *30*, 839–848.

Summerfield, M. A. (1991), *Global Geomorphology*, 537 pp., Prentice-Hall, Upper Saddle River, N. J.

Swanson, D. A. (1973), Pahoehoe flows from the 1969–1971 Mauna Ulu eruption, Kilaeuea volcano, Hawaii, *Geol. Soc. Am. Bull.*, *84*, 615–626.

Tobie, G., J. I. Lunine, and C. Sotin (2006), Episodic outgassing as the origin of atmospheric methane on Titan, *Nature*, *440*, 61–64.

Tokano, T., G. J. Molina-Cuberos, H. Lammer, and W. Stumptner (2001a), Modelling of thunderclouds and lightning generation on Titan, *Planet. Space Sci.*, *49*, 539–560.

Tokano, T., F. M. Neubauer, M. Laube, and C. P. McKay (2001b), Three-dimensional modeling of the tropospheric methane cycle on Titan, *Icarus*, *153*, 130–147.

Tomasko, M. G., et al. (2005), Rain, winds and haze during the Huygens probe's descent to Titan's surface, *Nature*, *438*, 765–778.

Toon, O. B., C. P. McKay, R. Courtin, and T. P. Ackerman (1988), Methane rain on Titan, *Icarus*, *75*, 255–284.

Wallace, J. M., and P. V. Hobbs (1977), *Atmospheric Science: An Introductory Survey*, Elsevier, New York.

West, R. A., M. E. Brown, S. V. Salinas, A. H. Bouchez, and H. G. Roe (2005), No oceans on Titan from the absence of a near-infrared specular reflection, *Nature*, *436*, 670–672.

Whipple, K. X. (2004), Bedrock rivers and the geomorphology of active orogens, *Annu. Rev. Earth Planet. Sci.*, *32*, 151–185.

Whipple, K. X., G. S. Hancock, and R. S. Anderson (2000), River incision into bedrock: Mechanics and relative efficacy of plucking, abrasion, and cavitation, *Geol. Soc. Am. Bull.*, *112*, 490–503.

Wilcock, P. R. (1992), Flow competence: A criticism of a classic concept, *Earth Surf. Processes Landforms*, *17*, 289–298.

World Meteorological Organization (1994), Guide to hydrologic practices, *WMO 168*, Geneva.

Yager, E., B. W. McArdell, W. E. Dietrich, and J. W. Kirchner (2005), Measurements of flow and sediment transport in a steep, rough stream, paper presented at General Assembly, Eur. Geosci. Union, Vienna.

Zarnecki, J. C., et al. (2005), A soft solid surface on Titan as revealed by the Huygens Surface Science Package, *Nature*, *438*, 792–795.

_____

M. Ádámkovics, Department of Astronomy, University of California, Berkeley, 601 Campbell Hall, Berkeley, CA 94720, USA.

I. Y. Fung, M. P. Lamb, J. T. Perron, and E. Yager, Department of Earth and Planetary Science, University of California, Berkeley, 307 McCone Hall, Berkeley, CA 94720, USA. (perron@eps.berkeley.edu)

C. D. Koven, Department of Environmental Science, Policy and Management, University of California, Berkeley, 137 Mulford Hall, Berkeley, CA 94720, USA.